Electronic Supplementary Material (ESI) for Nanoscale.
This journal is © The Royal Society of Chemistry 2024

SI: Effect of solvent quality and sidechain architecture on the conjugated polymer chain conformation in solution

Guorong Ma[1], Zhaofan Li[2], Lei Fang[3], Wenjie Xia[2], Xiaodan Gu[1*]

1. School of Polymer Science and Engineering, The University of Southern Mississippi, Hattiesburg, MS, 39406, USA

2. Department of Aerospace Engineering, Iowa State University, Ames, IA 50011, USA

3. Department of Chemistry, Texas A&M University, College Station, TX 77843, USA

Correspondence to: Xiaodan Gu (Email: xiaodan.gu@usm.edu)

Table of Contents

1 EXPERIMENT SECTION 2

1.1 Solution preparation 2
1.2 dn/dc measurement 2
1.3 HSP prediction 2
1.4 DSC measurement 2

2 SUPPORTING FIGURES AND TABLE 3

Figure S1 Photo of P3ATs solutions after aging at room temperature for 2 days. The concentration is 1.0 mg/ml. 3
Figure S2 DLS result of P3ATs at 20°C. (a, b) in THF and (c, d) in CF. The autocorrelation function and size distribution curve are shown in (a,c) and (b,d) respectively. The solution concentration is 1.0 mg/ml. 4
Figure S3 UV-Vis absorption spectrum of all CPs in CB (a) and in Tol (b) at 20°C. The spectrum of P3HT, P3OT, P3DT, and P3DDT are overlapped together. 4
Table S1 Wavelength at maximum absorption of all solutions at 20°C. 4
Figure S4 UV-Vis absorption spectrum of P3BT and P3HT in Tol (a, b) and CB (c, d) at various temperatures. Solution concentration is 0.1 mg/ml. 5
Table S2 Wavelength at maximum absorption of P3BT and P3HT Tol/CB solutions at various temperatures. 5
Figure S5 UV-Vis absorption spectrum of drop cast thin films of P3BT and P3HT from Tol and CB diluted solutions (0.1 mg/ml). The thin film was dried at room temperature overnight without thermal annealing. 6
Table S4 HSP value of P3HT, PQT-12, and PBTTT-12, based on HSP prediction from HSPiP software v5.4.07. 6
Figure S6 HSP value of solvent and P3HT. The arrow indicates the trend for increasing sidechain volume. Measured HSP values of P3HT are adapted from ref[1, 2]. 7
Figure S7 Debye plot of P3ATs in THF (a) and CF (b). 7
Figure S8 DSC result of P3HT, PQT-12 and PBTTT-12. Curves are from the second heating scan with a heating rate of 10K/min. 7
Figure S9 DLS evolution of P3HT solution 1.0 mg/ml after aging at r.t. for 10 days under dark conditions. Autocorrelation curve of P3HT in CB (a) and Tol (b), and particle size distribution in CB (c) and Tol (d) by NNLS fitting. 8
Figure S10 Sideview of an incidence laser beam (left) passing through a toluene solvent (a) and 0.04 mg/ml PffBT4T-C9C13 chlorobenzene solutions (b). (c) Photos of transmission laser projected on an A4 paper 1.5m away after passing through solution described in (b). 8
Figure S11 (a) Polymer architectures of type V and VI. (b-c) Reduced R_g of polymer chain as a function of solvent quality for type V to VI, respectively. 9
Figure S12 Normalized squared radius of gyration R_g^2 / (N - 1) as a function of solvent quality λ for polymer models I to VI, respectively, at higher temperatures. The location of the θ point is indicated by the black dashed line. 10
Figure S13 The persistence length L_p as a function of varying solvent quality λ for polymer models type I to VI, respectively. 11
Figure S14 Normalized squared end-to-end distance R_{ee}^2 / (N - 1) as a function of solvent quality λ for polymer models type I to VI, respectively. 12
Figure S15 The shape descriptor $\kappa 2$ as a function of varying solvent quality λ for polymer models type I to VI, respectively. 13

Figure S16 Molecular mass dependence of radius of gyration R_g for solvent qualities ranging from an ideal good solvent, θ solvent, to a poor solvent for seven types of polymer architectures. 14

REFERENCE 14

1 Experiment section

1.1 Solution preparation

Polymers were dissolved in filtered solvents and heated up to 80℃ overnight to ensure fully dissolved.

1.2 dn/dc measurement

20 mg CPs were dissolved in 1.0 ml solvents to obtain 20 mg/ml concentrated solution. Solution refractive index was measured by Abbe refractometry (Mettler Toledo Easy R40) at 20±0.1℃ and the differential refractive index was determined by the following equation.

$$\frac{dn}{dc} = \frac{n_{solution} - n_{solvent}}{c} \quad \text{Eq.1}$$

1.3 HSP prediction

HSP values for CPs and solvents are obtained from prediction in HSPiP software v5.4.07 shown in **Figure S6** and **Table S4**. Note that the predicted HSP value of P3HT does not match with the experimental value[1]. And no other P3ATs' HSP value has been measured and reported to the best of our knowledge.

1.4 DSC measurement

Differential scanning calorimetry (DSC) was performed in the Mettler Toledo 3+ DSC instrument. About 3 mg samples were sealed into an aluminum pan and the heating and cooling rate was 10 ℃/min under N_2 flow.

2 Supporting figures and table

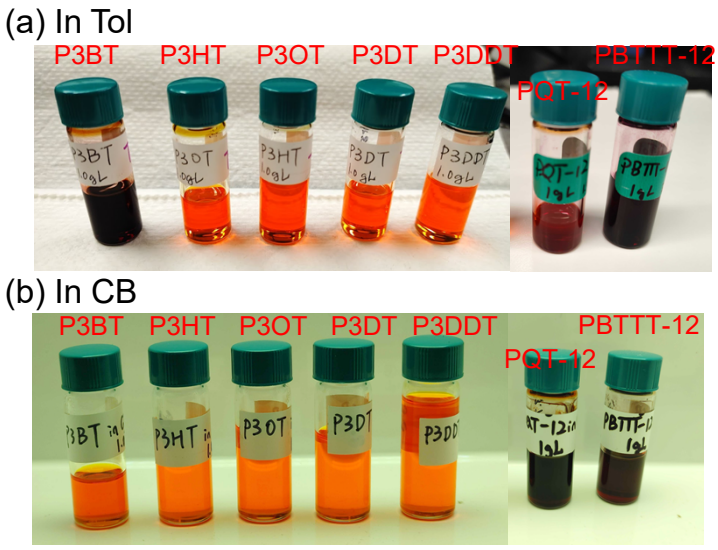

Figure S1 Photo of P3ATs solutions after aging at room temperature for 2 days. The concentration is 1.0 mg/ml.

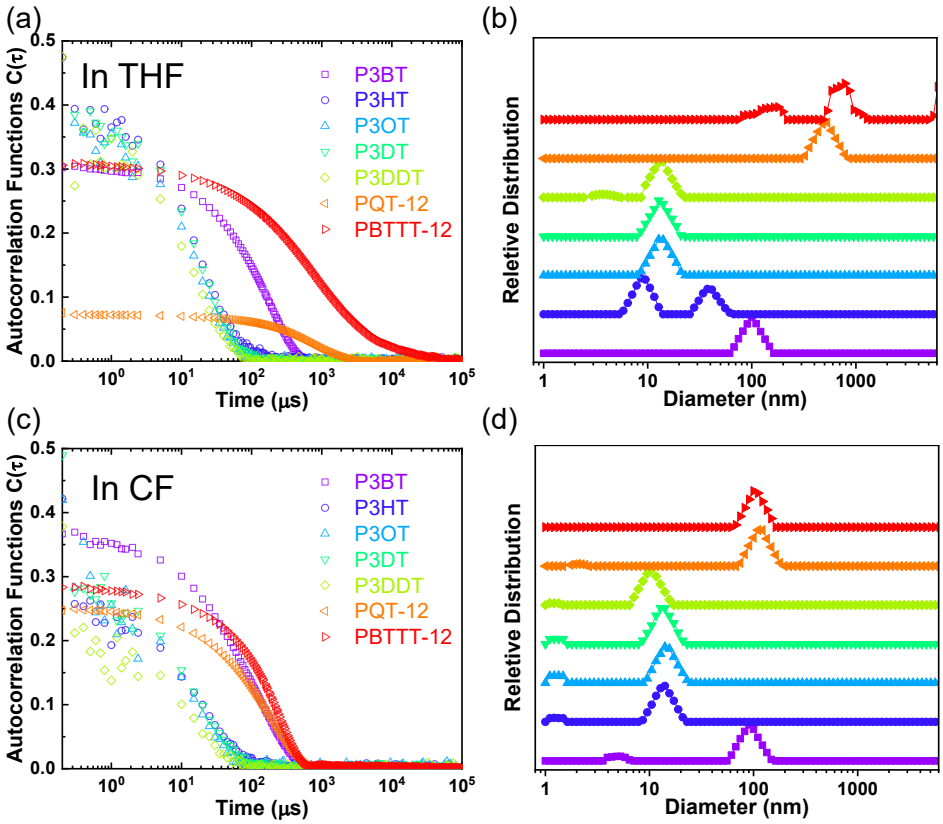

Figure S2 DLS result of P3ATs at 20℃. (a, b) in THF and (c, d) in CF. The autocorrelation function and size distribution curve are shown in (a,c) and (b,d) respectively. The solution concentration is 1.0 mg/ml.

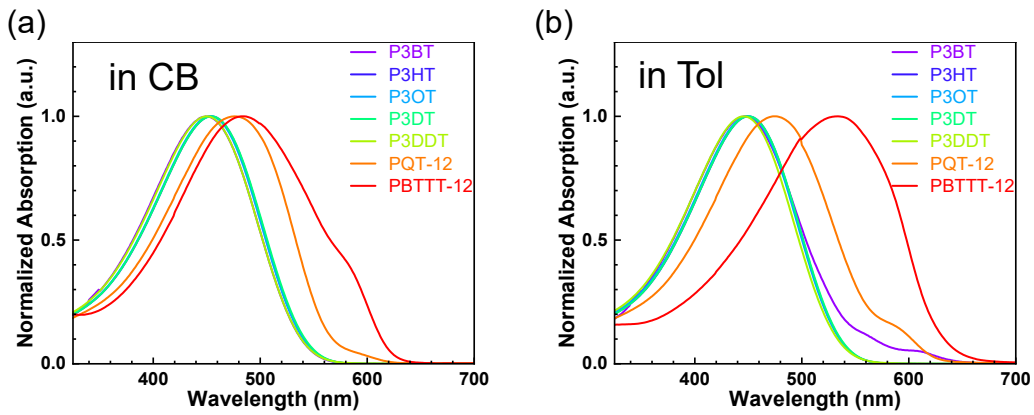

Figure S3 UV-Vis absorption spectrum of all CPs in CB (a) and in Tol (b) at 20℃. The spectrum of P3HT, P3OT, P3DT, and P3DDT are overlapped together.

Table S1 Wavelength at maximum absorption of all solutions at 20℃.

Name	**$\lambda_{max\ abs,\ CB}$/nm**	**$\lambda_{max\ abs,\ Tol}$/nm**
P3BT	449	446
P3HT	454	450
P3OT	453	449
P3DT	454	450
P3DDT	450	446
PQT-12	476	474
PBTTT-12	483	533

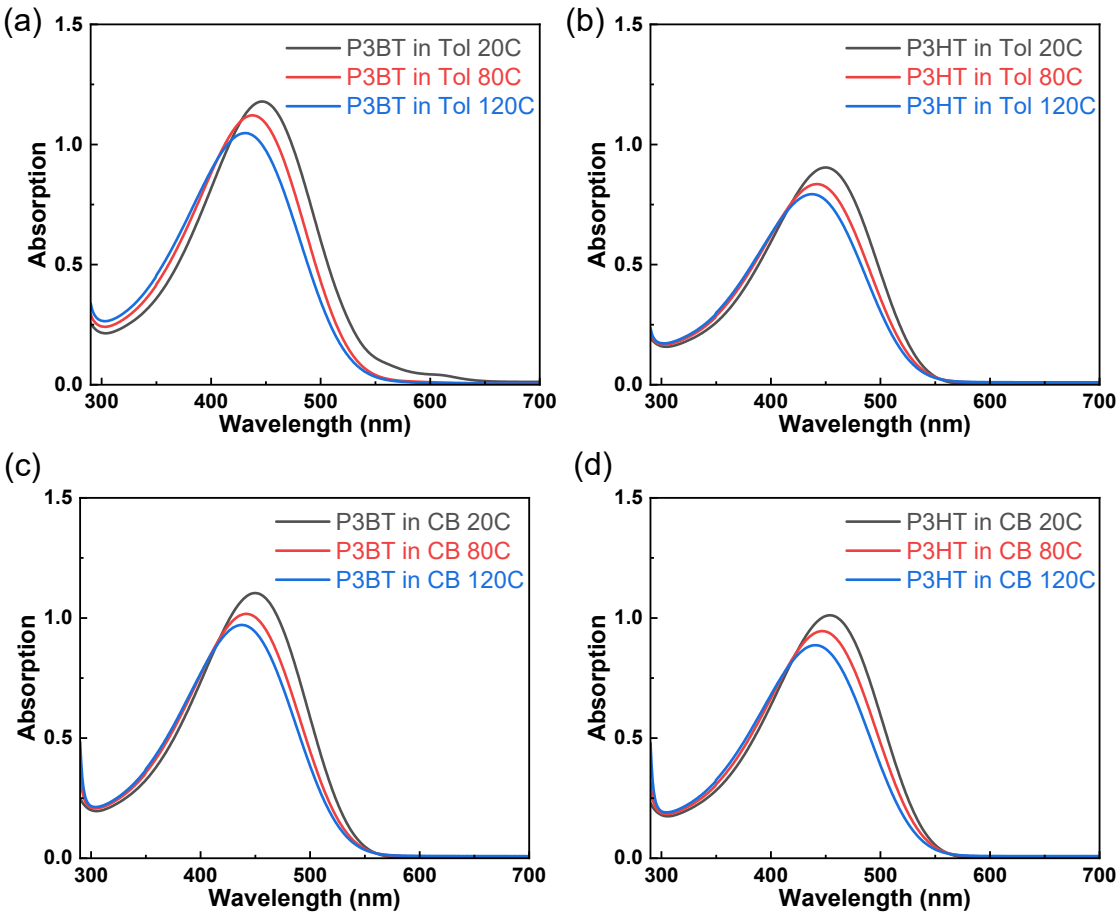

Figure S4 UV-Vis absorption spectrum of P3BT and P3HT in Tol (a, b) and CB (c, d) at various temperatures. Solution concentration is 0.1 mg/ml.

Table S2 Wavelength at maximum absorption of P3BT and P3HT Tol/CB solutions at various temperatures.

Polymer	**Temperature/ °C**	**$\lambda_{max\ abs,\ Tol}$/nm**	**$\lambda_{max\ abs,\ CB}$/nm**
P3BT	20	447	450
	80	438	442
	120	431	438
P3HT	20	450	454
	80	442	447
	120	437	441

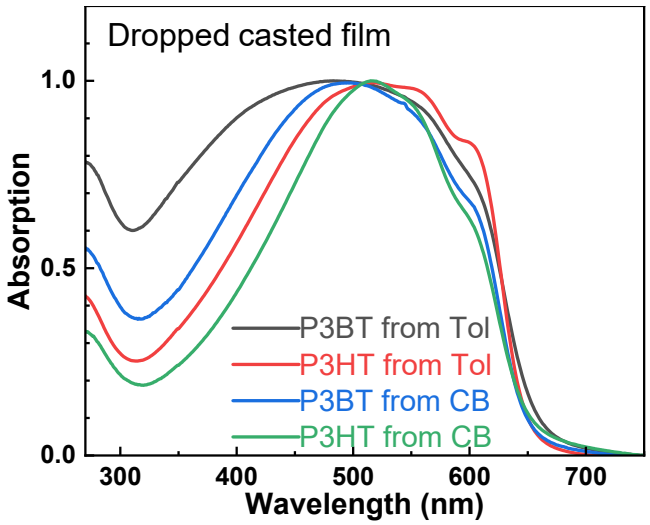

Figure S5 UV-Vis absorption spectrum of drop cast thin films of P3BT and P3HT from Tol and CB diluted solutions (0.1 mg/ml). The thin film was dried at room temperature overnight without thermal annealing.

Table S3 dn/dc value (at Na D line) and absorption coefficient (at 633nm) value of P3ATs in various solvents. *PQT-12 and PBTTT-12 are assumed to be the same as P3HT due to the difficulties of their measurement.

Polymer/ Solvent	dn/dc (ml/g)			
	CB	Toluene	THF	Chloroform
P3BT	0.280	0.225	0.465	0.365
P3HT	0.225	0.195	0.320	0.305
P3OT	0.175	0.200	0.420	0.295
P3DT	0.150	0.180	0.315	0.235
P3DDT	0.125	0.155	0.335	0.210
PQT-12*	0.225	0.195	0.320	0.305
PBTTT-12*	0.225	0.195	0.320	0.305

Table S4 HSP value of P3HT, PQT-12, and PBTTT-12, based on HSP prediction from HSPiP software v5.4.07.

Polymer Name		**P3HT**	**PQT-C12**	**PBTTT-C12**
Formula		$(C_{40}H_{56}S_4)n$	$(C_{40}H_{56}S_4)n$	$(C_{38}H_{56}S_4)n$
Prediction by HSPiP	δD	15.9	16.8	15.9
	δP	1.2	1.2	1.5
	δH	2.1	2.1	1.8

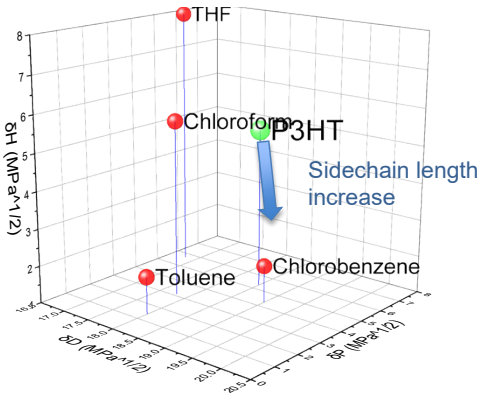

Figure S6 HSP value of solvent and P3HT. The arrow indicates the trend for increasing sidechain volume. Measured HSP values of P3HT are adapted from ref[1, 2].

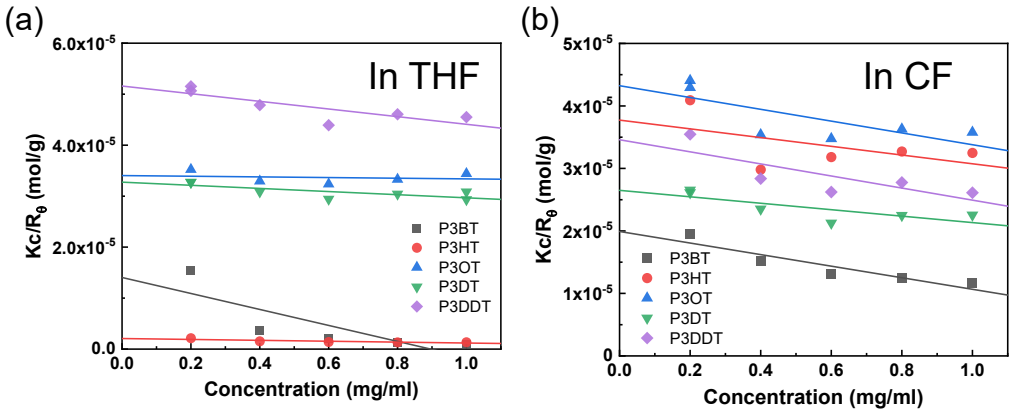

Figure S7 Debye plot of P3ATs in THF (a) and CF (b) at 20℃.

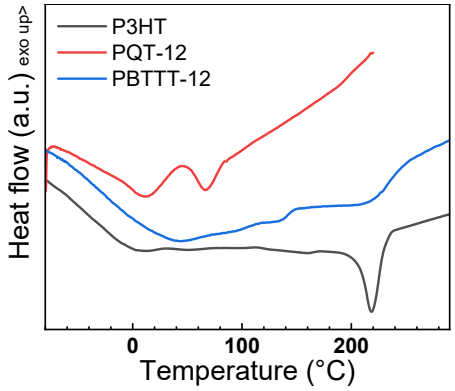

Figure S8 DSC result of P3HT, PQT-12 and PBTTT-12. Curves are from the second heating scan with a heating rate of 10K/min.

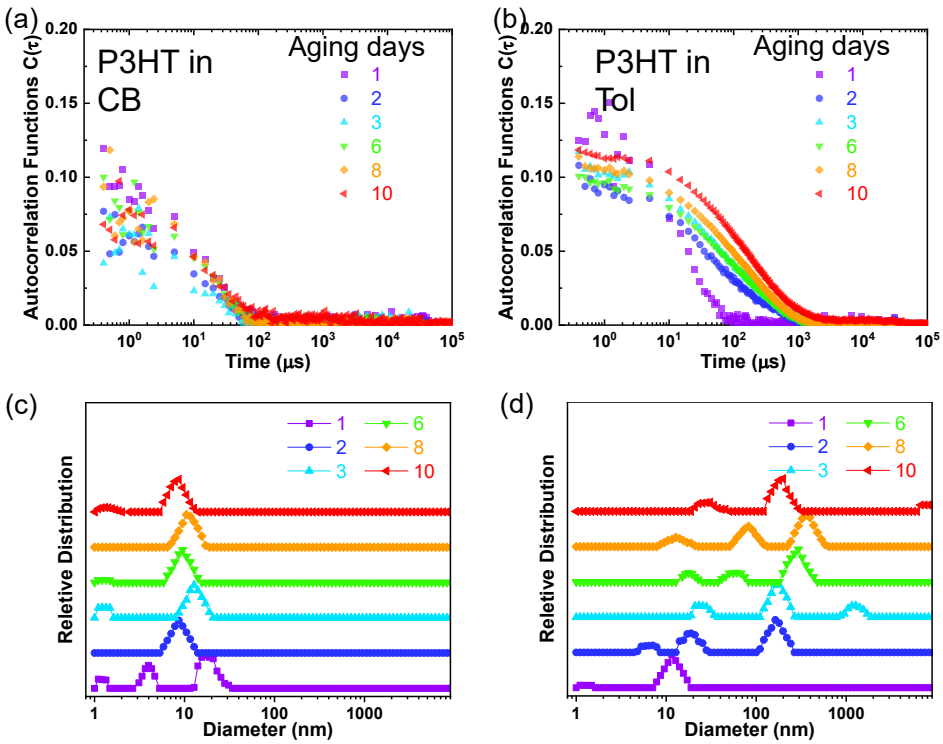

Figure S9 DLS evolution of P3HT solution 1.0 mg/ml after aging at r.t. for 10 days under dark conditions. Autocorrelation curve of P3HT in CB (a) and Tol (b), and particle size distribution in CB (c) and Tol (d) by NNLS fitting.

Figure S10 Sideview of an incidence laser beam (left) passing through a toluene solvent (a) and 0.04 mg/ml PffBT4T-C9C13 chlorobenzene solutions (b). (c) Photos of transmission laser projected on an A4 paper 1.5m away after passing through solution described in (b).

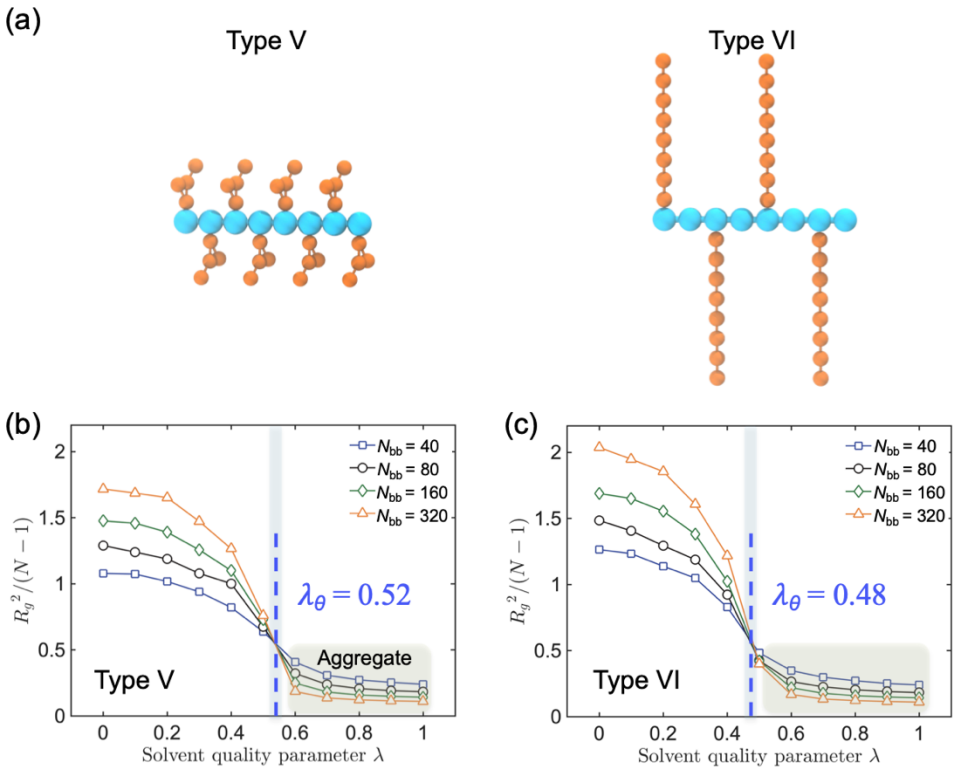

Figure S11 (a) Polymer architectures of type V and VI. (b-c) Reduced R_g of polymer chain as a function of solvent quality for type V to VI, respectively.

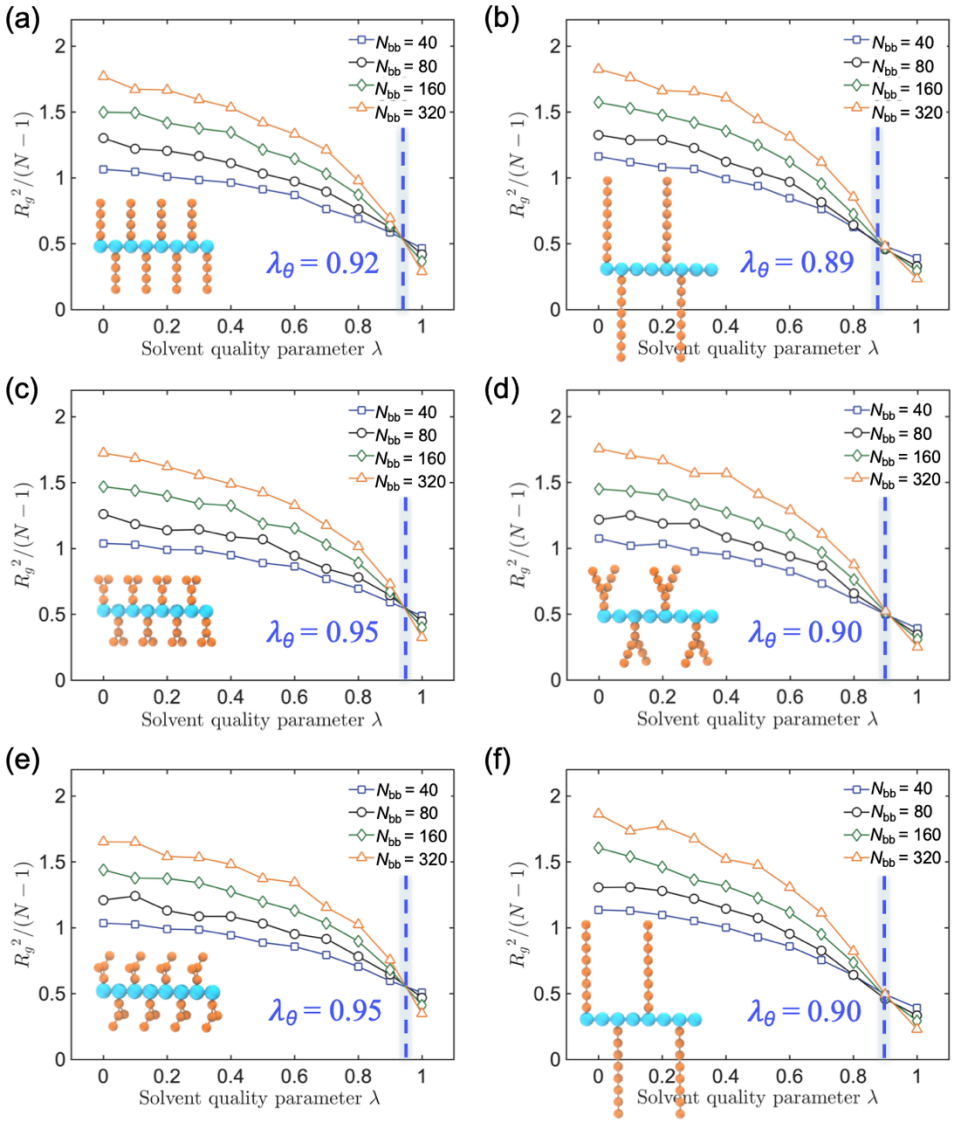

Figure S12 Normalized squared radius of gyration R_g^2 / (N - 1) as a function of solvent quality λ for polymer models I to VI, respectively, at higher temperatures. The location of the θ point is indicated by the black dashed line.

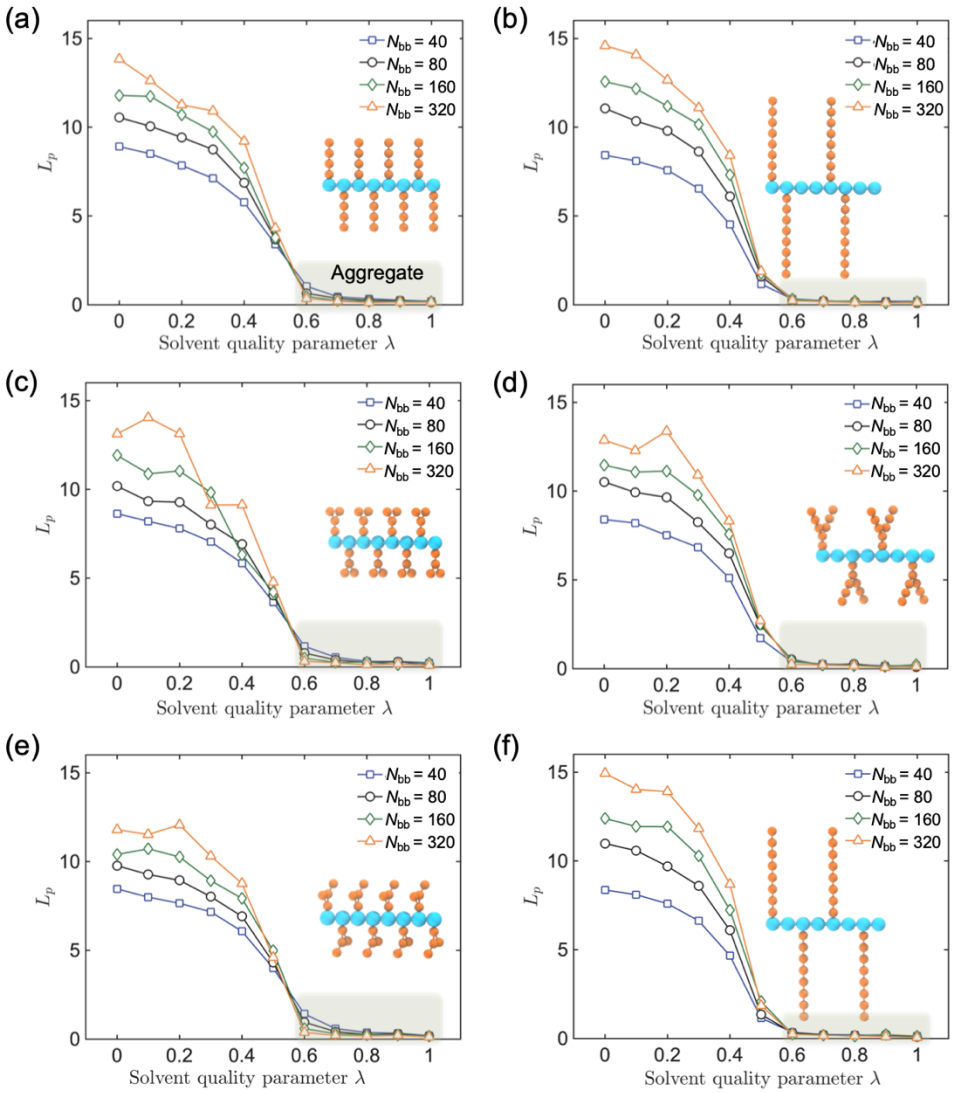

Figure S13 The persistence length L_p as a function of varying solvent quality λ for polymer models type I to VI, respectively.

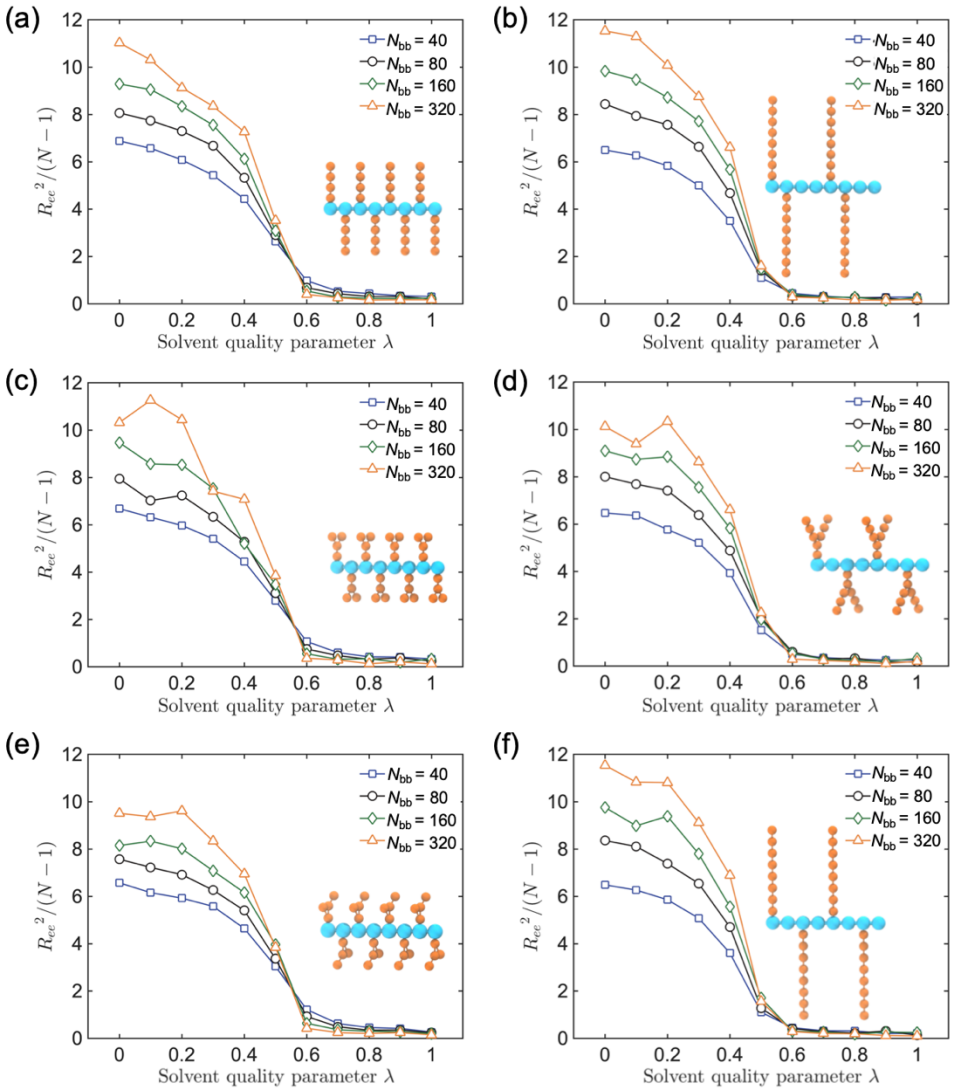

Figure S14 Normalized squared end-to-end distance R_{ee}^2 / (N - 1) as a function of solvent quality λ for polymer models type I to VI, respectively.

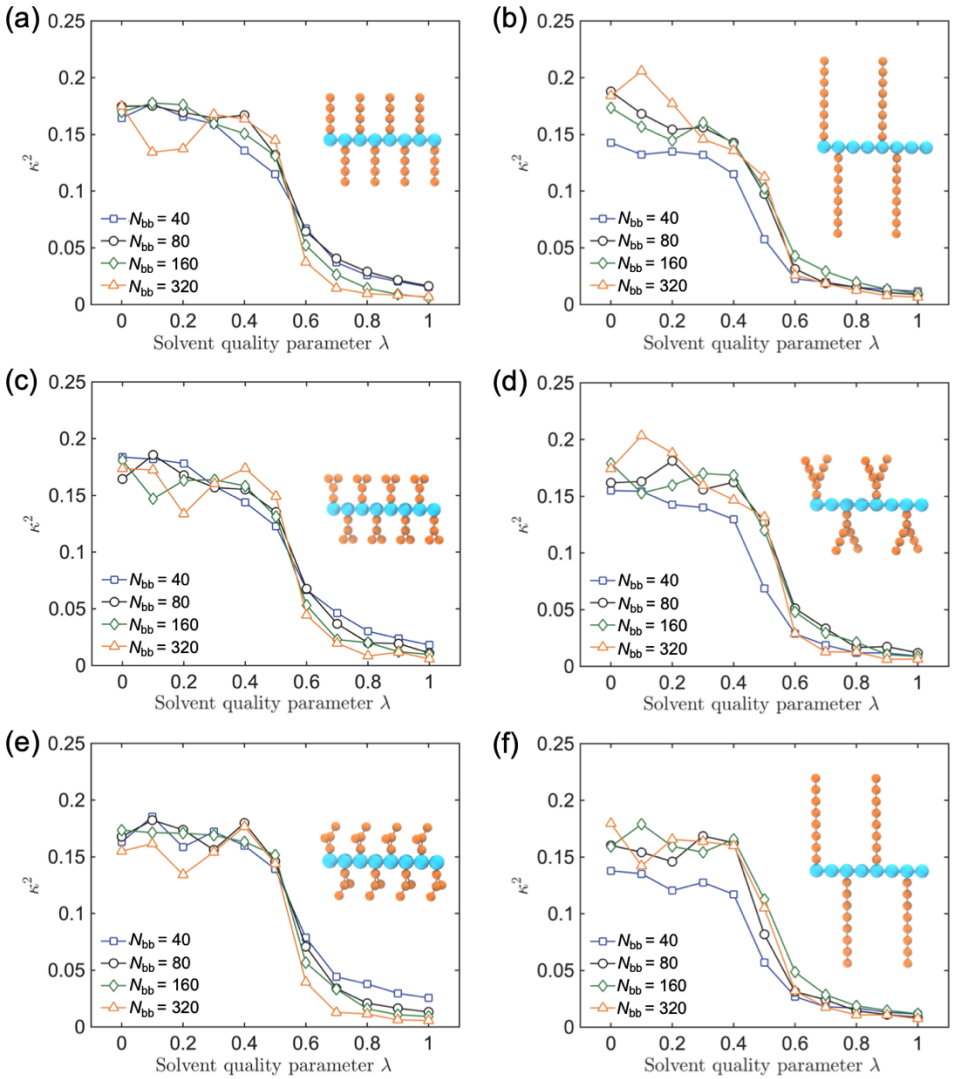

Figure S15 The shape descriptor κ^2 as a function of varying solvent quality λ for polymer models type I to VI, respectively.

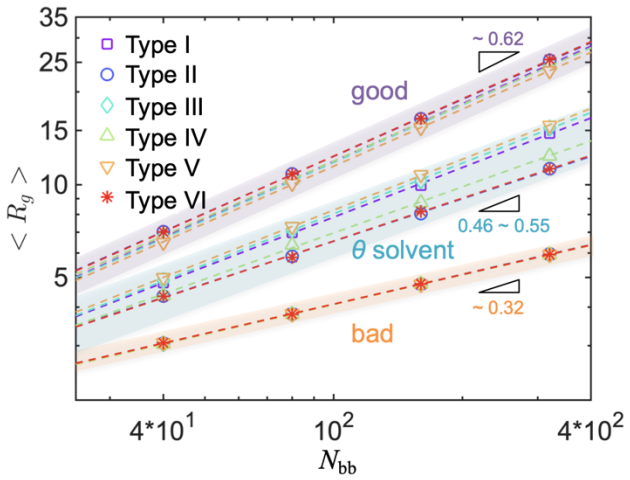

Figure S16 Molecular mass dependence of radius of gyration R_g for solvent qualities ranging from an ideal good solvent, θ solvent, to a poor solvent for seven types of polymer architectures.

Reference

1. Machui, F.; Langner, S.; Zhu, X. D.; Abbott, S.; Brabec, C. J. Determination of the P3HT:PCBM solubility parameters via a binary solvent gradient method: Impact of solubility on the photovoltaic performance. *Sol. Energy Mater. Sol. Cells* **2012,** 100, 138-146 DOI: 10.1016/j.solmat.2012.01.005.

2. Machui, F.; Abbott, S.; Waller, D.; Koppe, M.; Brabec, C. J. Determination of Solubility Parameters for Organic Semiconductor Formulations. *Macromol. Chem. Phys.* **2011,** 212 (19), 2159-2165 DOI: 10.1002/macp.201100284.